

Cellular-automaton approach to two-dimensional VCSEL array collective behaviour (*)

F. PREVIDI⁽¹⁾ and M. MILANI⁽²⁾

⁽¹⁾ *Dipartimento di Elettronica e Informazione, Politecnico di Milano
via Ponzio 34/5, 20133 Milano, Italy
INFN, Sezione di Milano - Milano, Italy*

⁽²⁾ *Dipartimento di Scienza dei Materiali, Università di Milano
via Emanueli 15, 20126 Milano, Italy
INFN, Sezione di Milano - Milano, Italy*

(ricevuto il 16 Marzo 1998; approvato il 24 Luglio 1998)

Summary. — A Cellular Automaton (CA) is used for modelling a two-dimensional array of single-mode Vertical Cavity Surface Emitting Laser (VCSEL). Preliminary results are reported on the dynamics of generation of collective array supermodes. In particular, coupling of devices has been computed at different values of injection current; the time evolution of cross-talk among devices has been successfully simulated even in the case of the presence of a damaged device; fundamental supermode far-field emission pattern is reported in good agreement with other analytical approaches and experimental results. The reduced computational cost and the chance of merging physical parameters with geometrical topologies make the CA models a useful and powerful complement to classical analytical modelling of complex interacting optical-device collections.

PACS 42.79 – Optical elements, devices, and systems.

PACS 42.55.Px – Semiconductor lasers; laser diodes.

PACS 42.25 – Wave optics.

1. – Introduction

Since their first development [1], VCSELs have generated a great interest for their possible applications, in particular when used in two-dimensional configurations. The realization of two-dimensional arrays in which the single devices are phase-locked in order to produce a coherent beam is very attractive for the realization of optical memories or other similar devices. Actually, it is possible to obtain very high densely packed two-dimensional arrays of VCSELs (less than 1 mm radius devices, about 0.2 mm between lasing elements) [2-5] with very low threshold current (about 100 mA) [2, 3, 6-8] and high power conversion efficiency [6-8]. In such arrays it is necessary to consider the coupling properties of each device. Array supermode analysis

(*) The authors of this paper have agreed to not receive the proofs for correction.

is possible via analytical calculations [9, 10], but symmetry requirements are needed for supermode computation and the effects of possible electric coupling are also to be taken into account.

In this work the collective behaviour of single-mode devices of a very high densely packed array will be modelled using a single Cellular Automaton (CA) [11, 12]; in particular, array fundamental supermode near-field and far-field emission patterns have been obtained. This is a preliminary result on the way towards the prediction of other supermodes, which emerge as current increases, and of the mechanism of generation of array coherent emission, in order to realize devices optimized for very high output power. Furthermore, the CA technique is very effective in describing the dynamic of cross-talk diffusion in the array and in predicting coupling degree of devices at different injection currents.

CA are powerful tools for the interpretation of real-device behaviours, since they can take into account non-homogeneity, aging of the lasers in the array and the possible irreversible damaging of an element [13-15]. Moreover, the CA approach allows a suitable description of any two-dimensional geometry, from those with a high degree of spatial regularity (periodic arrays) to those strongly asymmetric covering a wide range in the element numbers.

2. – The model and the underlying physics

A CA is supported by a cellular space, *i.e.* an ensemble of cells (in our case the wafer supporting the array [6]); it is defined by five properties: the *cellular space topology* (how cells are arranged); the cell *neighbourhood*; the cell *state space*; the *transition rules* which describe the temporal evolution of the cell state and so the global state evolution of the whole automaton (which is not merely the ensemble of the states of the single cells); in the transition rules an (external, non-symmetric or with symmetry different from those of the array) *exogenous input* can be inserted too.

In this work the *cellular space* is a two-dimensional squared array of cells even if this hypothesis can be relaxed; each cell represents a single-mode VCSEL.

The *neighbourhood* of the generic cell in the position (i, j) is defined as follows:

$$(1) \quad U(i, j) = \{(i - 1, j)(i + 1, j)(i, j - 1)(i, j + 1)\},$$

i.e. the lattice is a squared one (a possible extension can be the hexagonal one that could be a useful approach to strained wafers).

The *state space* is the ensemble of the single-cell states; it is the set $P = \{0, 1, -1\}$. This choice derives from the possible interlinked physical states of the laser.

The state $p = 0$ represents a VCSEL in the state “off” (below threshold); the state $p = 1$ represents a VCSEL in the state “on” (beyond threshold) with zero phase of the emitted field; the state $p = -1$ corresponds to a VCSEL emitting field π out of phase with respect to the previous one.

In a unit time step the following rules take place and must be accounted for:

– a current is injected in each VCSEL of the array and undergoes fractionation: an amount of this current is dispersed in the array (it will be taken into account as joule heating in a further release) and a first part of the remaining one is converted into light: this conversion, described by a characteristic *I-L* curve, is ruled by the coefficient (differential quantum efficiency) $\eta_{i,j}^k$, where i, j indicate the position of the laser in the

array and k are the unit time steps that have elapsed; the second part is (uniformly) spread off towards the nearest VCSELs (current leakage): this loss is ruled by the *current leakage coefficient* $a_{i,j}^k$.

– if the current in a device is enough, *i.e.* it overcomes a threshold, laser light emission starts. Since devices in the array are very close, the emitted fields of two adjacent lasers could overlap. In the fundamental supermode the fields emitted by adjacent lasers are π out of phase (*i.e.* the array is in its minimum-energy configuration) and the field interaction is destructive, *i.e.* the overlapping effect is field intensity decreasing; so this phenomenon is ruled by the *field leakage coefficient* $b_{i,j}^k$ in strict analogy with current leakage.

Field overlapping can be computed also with other techniques [10] using the analogy of field confinement in laser cavity with optical fibres. The advantage of CA approach is that it takes into account both physical and geometric aspects of coupling, *i.e.* the typical dimension of the laser (radius), the dependence on the ratio between radius and laser distance and the material support of the device (so it is not necessary to build different families of curves as cladding material changes).

The current circulating in the device at the position (i, j) at the time $t = k + 1$ (or seen as the normalised electron number present in the single device at time $t = k + 1$) is

$$(2) \quad e_{i,j}^{k+1} = \left(\frac{a_{i-1,j}^k}{4} e_{i-1,j}^k + \frac{a_{i+1,j}^k}{4} e_{i+1,j}^k + \frac{a_{i,j-1}^k}{4} e_{i,j-1}^k + \frac{a_{i,j+1}^k}{4} e_{i,j+1}^k + u_{i,j}^{k+1} \right),$$

where $e_{i-1,j}^k, e_{i+1,j}^k, e_{i,j-1}^k, e_{i,j+1}^k$ are the currents circulating in the neighbour cells at the time $t = k$; $u_{i,j}^{k+1}$ is the current injected in the VCSEL in the position (i, j) at the current time.

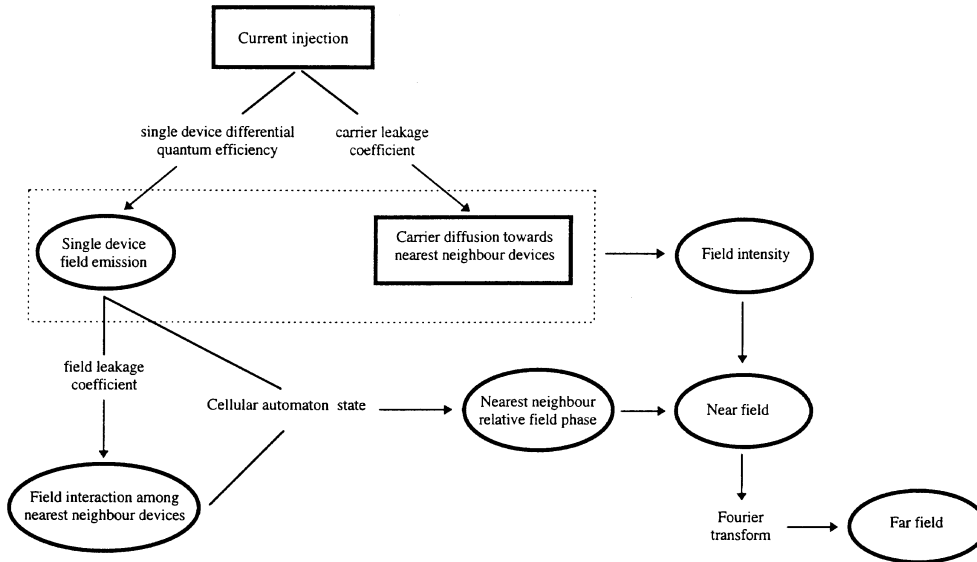


Fig. 1. – Schematic sketch of the radiation-matter interaction as simulated in an elementary time step computed by the cellular automaton.

Then the light emitted is computed as photon number in unit time:

$$(3) \quad p_{i,j}^{k+1} = \eta_{i,j}^{k+1} (1 - a_{i,j}^{k+1}) e_{i,j}^{k+1} + \\ + A_{i,j} \left(A_{i-1,j} \frac{b_{i-1,j}^k}{4} p_{i-1,j}^k + A_{i+1,j} \frac{b_{i+1,j}^k}{4} p_{i+1,j}^k + A_{i,j-1} \frac{b_{i,j-1}^k}{4} p_{i,j-1}^k + A_{i,j+1} \frac{b_{i,j+1}^k}{4} p_{i,j+1}^k \right),$$

where $\eta_{i,j}^{k+1} e_{i,j}^{k+1}$ is the part due to injection current in the laser and

$$A_{h,k} = \begin{cases} 1 & \text{if the state of the cell in the position } (h, k) \text{ is } p \neq 0, \\ 0 & \text{otherwise.} \end{cases}$$

If $e_{i,j}^{k+1} > (e_{i,j}^{k+1})_{\text{th}}$ or $p_{i,j}^{k+1} > (p_{i,j}^{k+1})_{\text{th}}$, the cell goes in one of the two states $p = \pm 1$ and arranges in order to minimize energy. Above, $(e_{i,j}^{k+1})_{\text{th}}$ represents the threshold current and $(p_{i,j}^{k+1})_{\text{th}}$ represents the possibility that field leakage switches on a neighbour laser. In fig. 1 a sketch of the automaton evolution rules as computed during an elementary time step is shown.

Boundary conditions are a very critical point for any kind of model and in particular for a statistical model as a cellular automaton [16]; the rules for the cells at the array boundary have been assumed by supposing the existence of perfect diffusion conditions, both for charge carriers and for emitted field.

In our notation we show the possibility to extend such a model leaving cellular automata domain, *i.e.* the temporal locality can be relaxed and/or the spatial locality, allowing the coefficients η , a , b not to be fixed either spatially or temporally, so that they can be different for any device in the array, and they can follow any desired temporal law. This novel net structure lacks the regular and simple computational capability of a cellular automaton, but it can describe a more various set of situations; on the other hand it does not always grant the possibility of describing the stable mesostructures of the array emission as a cellular automaton will do.

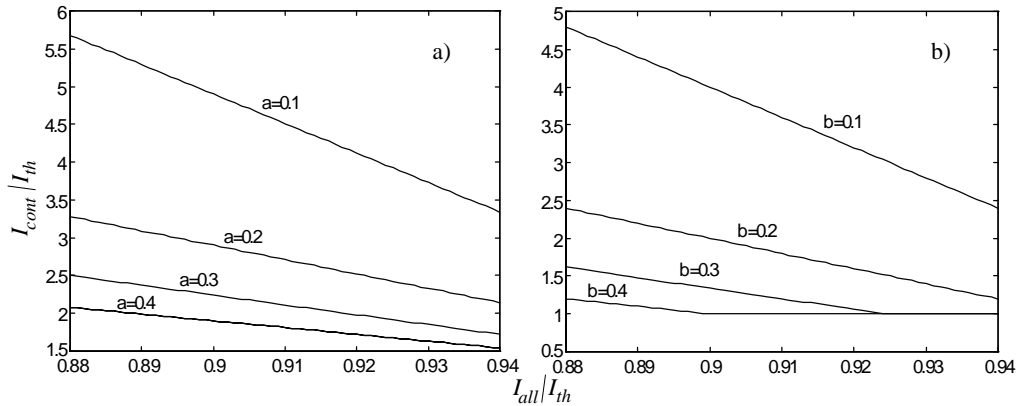


Fig. 2. – a) Current leakage due to carrier diffusion. Each curve is plotted for a given value of the a parameter. Below the curve leakage diffusion due to electric pathway is not possible. b) Field leakage due to field interference of neighbour devices. Each curve is plotted for a given value of the b parameter. Below the curve leakage diffusion due to optical pathway is not possible.

3. – Simulation results

The following simulations have been developed using a CA for modelling a squared array of identical VCSELs, so that all devices in the array have the same threshold current and the leakage parameters are homogeneous throughout the whole array.

A large number of simulations have been carried on in order to characterize the two different leakage mechanisms; all of them have been made following the same procedure: all the lasers of the array are brought in a pre-bias condition at the current I_{all} ; at the same time the current of one of the devices is slowly increased until leakage is enough to light on first-neighbour devices: the current at which this phenomenon occurs is called *control current* and it is named I_{cont} .

In figs. 2 and 3, I_{cont} vs. I_{all} has been plotted for different values of leakage parameters and some curves have been obtained: above them leakage is occurring in

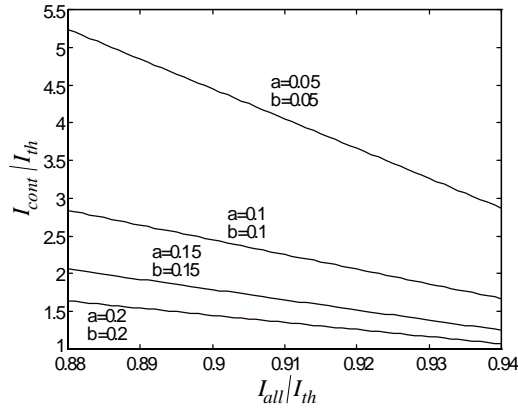


Fig. 3. – Effect of both pathways' leakage superposition.

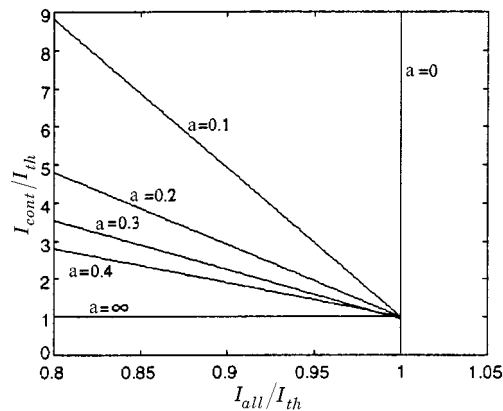


Fig. 4. – Current leakage extrapolation from simulations. Notice the extrapolated curves corresponding to the values $a = 0$ and $a = \infty$ which are in agreement with the threshold behaviour of the array. A similar plot is possible also for optical cross-talk and for superposition of electric and optic pathways.

the array. In fig. 2a) only the current leakage pathway is on; in fig. 2b) field leakage only; in fig. 3 both leakage pathways are active.

Notice that in fig. 2b) the simulation prediction is consistent with the device threshold behaviour. In particular, the meaning of this result is that over a certain pre-bias current value it is enough to bring a single device slightly over threshold to have significant leakage between devices. This cannot occur along current

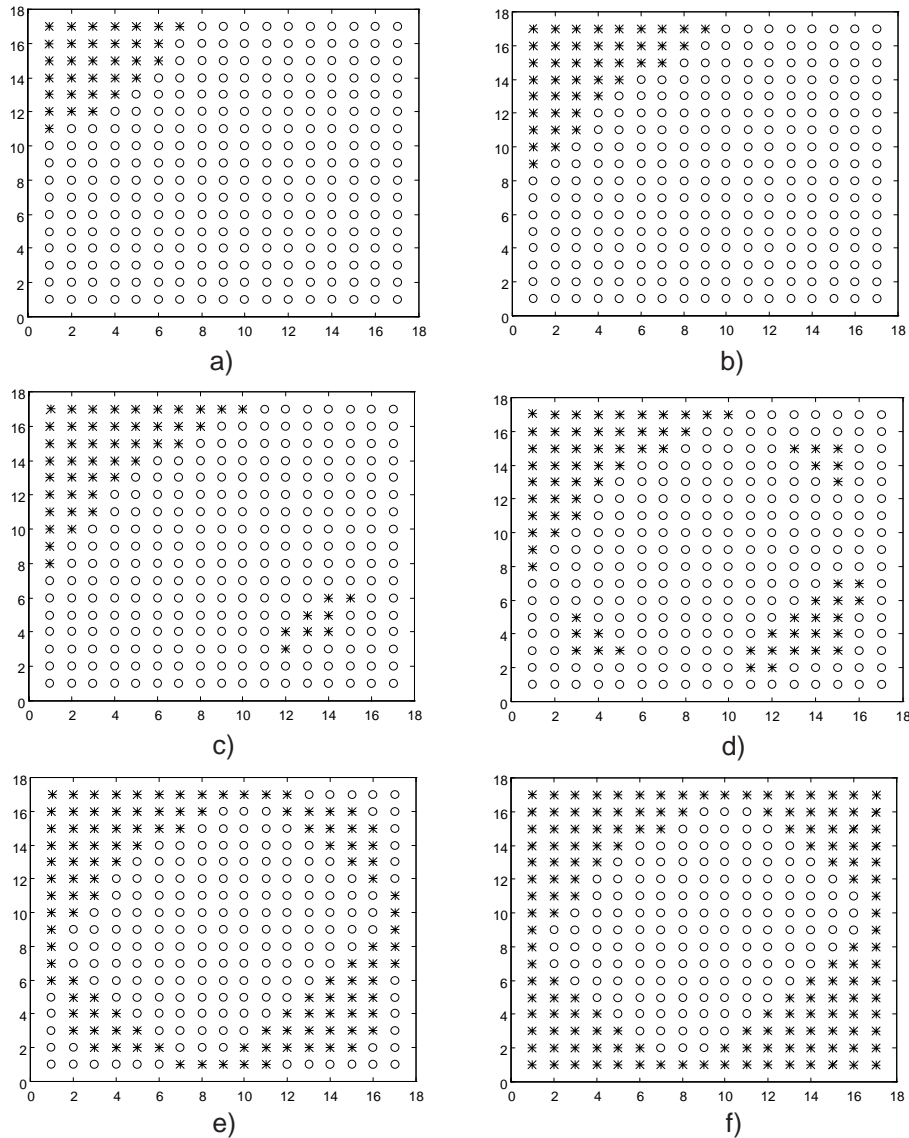


Fig. 5. – Dynamic of leakage: the interaction diffusion process in the array in the particular case of an array with a damaged laser in its central position; one can notice the information on the range of the interaction. a) Time step $k = 13$; b) time step $k = 19$; c) time step $k = 20$; d) time step $k = 21$; e) time step $k = 22$; f) time step $k = 25$.

leakage path as can be seen by fig.4, showing an extrapolation by simulation results.

This CA procedure can be applied to real devices in order to estimate the lasers degree of coupling and the whole array threshold current as predicted by the CA, which is usually less than the simple sum of the threshold currents for the elemental devices.

The correlation of the cellular-automaton model parameters with a real device with its own geometry and material properties can be carried out performing on the array a set of measures in the way described before; so doing, it is possible to obtain the a , b , h model parameters and then to make the cellular automaton run in order to obtain predictions on the device emission properties. For instance, from the whole array characteristic curves of figs.3 and 4 with $a = 0.05$ and $b = 0.05$, it is possible to estimate, for a 17×17 array with single-device threshold current of about 1.5 mA, an array threshold current of about 390 mA, with an 11% reduction with respect to the sum of the devices threshold currents [17].

The CA technique also allows to take into account possible non-homogeneous features of device arrays: a quantitative evaluation is obtained of the reduction of the total threshold current caused by collective effects in the array (cooperation).

Heating effects can be omitted, since it can be assumed that the array is operating with 100 ns pulses at a rate of about 10 kHz; it has been experimentally verified [17] that heating in these conditions is under control and every property of the array can be examined since all dynamics are typically ten times faster.

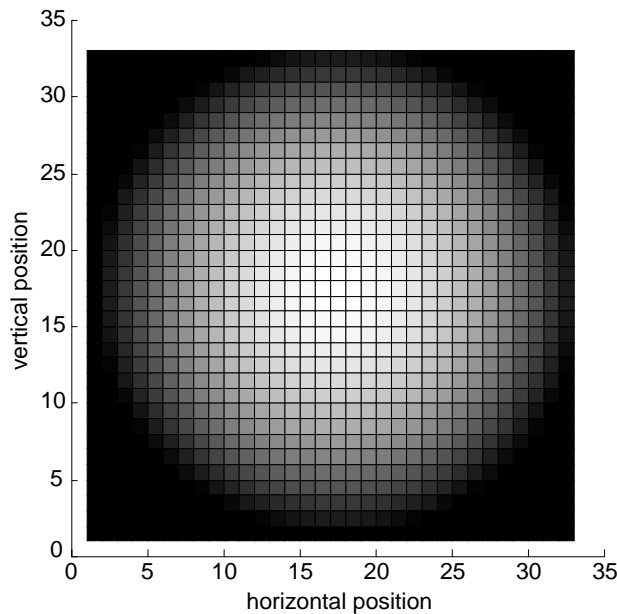


Fig. 6. – Near-field emission pattern in grey scale of colours. This pattern has been obtained from a 60 s simulation on a 486 PC on a 32×32 cellular automaton, with $a = 0.1$; $b = 0.1$. On the axis the vertical and horizontal position of devices in the array are reported. Grey scale intensity is normalized so that the less emitting laser is black and the most emitting is white.

Cellular Automata technique allows to follow the dynamics of leakage onset and its propagation in the array. In fig. 5 we show the interesting case of leakage diffusion process dynamics when one of the lasers is under the corresponding curve I_{cont} vs. I_{all} and so it is not able to propagate interaction. The array is composed of 17×17 identical devices; both current and field leakages are active: $a = 0.1$, $b = 0.1$. All devices have current 0.9 times the threshold current. The laser in position (17, 1) (upper left) has current which is 4 times the threshold one; the laser in position (9, 9) has current which is 0.88 times the threshold one. At the time step $k = 1$ the cellular automaton starts and the interaction diffusion process begins.

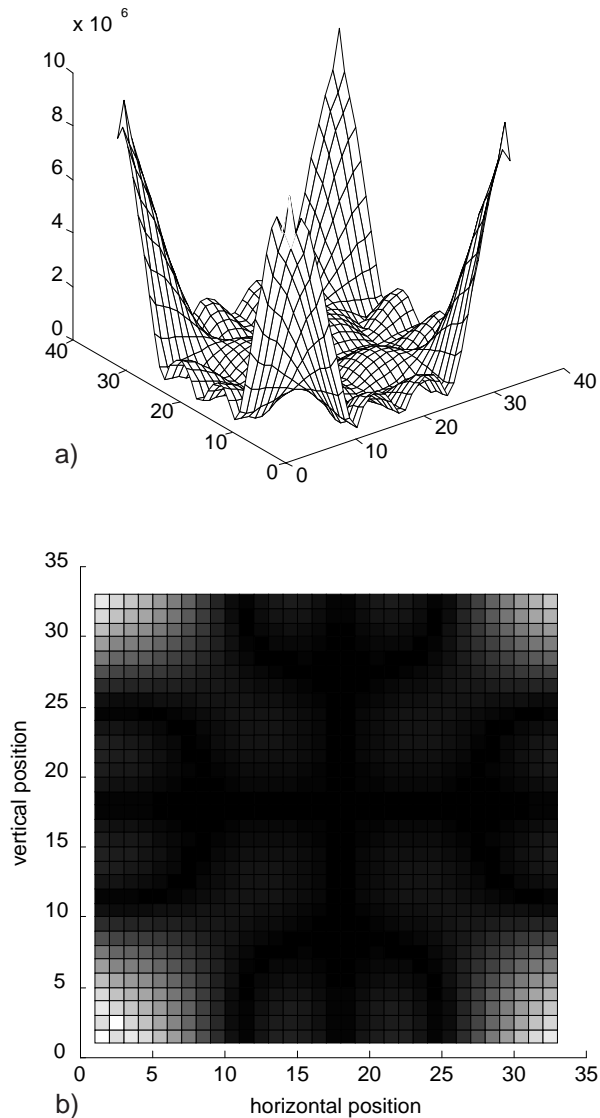


Fig. 7. – a) Three-dimensional view, in arbitrary units, of far-field emission pattern as simulated from cellular automaton. b) Plane projection of a) with a grey scale normalization as in fig. 6.

This simulation allows to obtain information on the range of the electric interaction between devices. In first approximation, the diffusion length of electrons is about 1 mm in not too heavily doped GaAs. Indeed, $L_n = \sqrt{D_n \tau_n}$, where D_n is the diffusion coefficient with typical value from 1 to 10 $\text{cm}^2 \text{s}^{-1}$ and τ_n is the overall electron recombination time with a typical value of 10^{-9} s, so the diffusion length ranges from 1 to 10 mm, *i.e.* over about four or five devices with 2 mm radius and 2.5 mm center-to-center distance as is visible in fig. 5.

The CA technique allows to describe the out-of-phase fundamental supermode emission pattern, since it directly furnishes the emitted field of each laser in the array. In fig. 6 the (normalized) emitted light intensity is visible as it is directly computed in about 20 elementary time steps.

The emitted-field phase, as just said, has been imposed in the automaton structure so that each device is out of phase with all the neighbours; the Fourier transform (computed with a FFT algorithm) of near-field emission is visible in fig. 7. In so doing, a simulation of far-field emission pattern is available in less than 60 s of simulation on a 486 PC.

4. – Conclusions

It has been shown that the CA approach gives a straightforward technique to handle dynamic time evolution and coherence appearance. In particular, the role of current leakage, field leakage and laser damaging can be directly related to global threshold prediction. Moreover, the fundamental supermode build-up can be evaluated in good agreement with experimental results. Finally, diffusive processes of laser interaction can be investigated in detail giving a clue to monitor array inhomogeneities.

REFERENCES

- [1] IGA K., KOYAMA F. and KINOSHITA S., *IEEE J. Quantum Electron.*, **24** (1988) 1845.
- [2] HUFFAKER D. L., GRAHAM L. A. and DEPPE D. G., *IEEE Photon. Technol. Lett.*, **8** (1996) 596.
- [3] HUFFAKER D. L. and DEPPE D. G., *IEEE Photon. Technol. Lett.*, **8** (1996) 858.
- [4] YOO H.-J., SCHERER A., HARBISON J. P., FLOREZ L. T., PAEK E. G., VAN DER GAAG B. P., HAYES R., VON LEHMEN A., KAPON E. and KWON Y.-S., *Appl. Phys. Lett.*, **56** (1990) 1198.
- [5] GOURLEY P. L., WARREN M. E., HADLEY G. R., VAWTER G. A., BRENNAN T. M. and HAMMONS B. E., *Appl. Phys. Lett.*, **58** (1991) 890.
- [6] CHOQUETTE K. D., SCHNEIDER R. P., LEAR K. L. and LEIBENGUTH R. E., *IEEE J. Select. Topics in Quantum Electron.*, **2** (1995) 661.
- [7] LEAR K. L., CHOQUETTE K. D., SCHNEIDER R. P. jr., KILCOYNE S. P. and GEIB K. M., *Electron. Lett.*, **31** (1995) 208.
- [8] HAYASHI Y., MUKAIHARA T., HATORI N., OHNOKI N., MATSUTANI A., KOYAMA F. and IGA K., *Electron. Lett.*, **31** (1995) 560.
- [9] YOO H.-J., HAYES J. R., PAEK E. G., SCHERER A. and KWON Y.-S., *IEEE J. Quantum Electron.*, **26** (1990) 1039.
- [10] YOO H.-J., HAYES J. R. and KWON Y.-S., *Electron. Lett.*, **26** (1990) 896.

- [11] WOLFRAM S., *Universality and complexity in Cellular Automata*, in *Proceedings of an Interdisciplinary Workshop*, edited by D. FARMER, T. TOFFOLI and S. WOLFRAM (North-Holland Physics Publishing) 1983, reprinted from *Physica D*, **10** (1984) 117.
- [12] BENNET C. H., TOFFOLI T. and WOLFRAM S., *Cellular Automata 1986 Conference* (M.I.T., Boston) 1986.
- [13] MILANI M., CATTANEO G., MAGNI F. and RIGOTTI M., *Nuovo Cimento B*, **111** (1996) 863.
- [14] MILANI M., CASATI R., CATTANEO G., MAGNI F. and SPINOGLIO L., *Cellular Automaton approach to semiconductor laser behaviour and applications*, in *Functional Photonic Integrated Circuits*, edited by M. N. ARMENESE and K. WONG, *Proc. SPIE*, **2401** (1995) 2408.
- [15] MILANI M., COSTATO M., BRIVIO F., CASATI R., CATTANEO G., MAGNI F., PISTONI N. C., PREVIDI F. and SPINOGLIO L., *A critical analysis of radiation-matter interaction*, submitted to *Rivista del Nuovo Cimento*.
- [16] WOLFRAM S., *Rev. Mod. Phys.*, **55** (1983) 601.
- [17] CATCHMARK J. M., ROGERS L. E., MORGAN R. A., ASOM M. T., GUTH G. D. and CHRISTODOULIDES D. N., *IEEE J. Quantum Electron.*, **32** (1996) 986.